J Mater Sci: Mater Med (2009) 20:597–606
DOI 10.1007/s10856-008-3600-5

Excimer laser chemical ammonia patterning on PET film

G. Wu · M. D. Paz · S. Chiussi · J. Serra · P. González · Y. J. Wang · B. Leon

Received: 29 December 2007 / Accepted: 23 September 2008 / Published online: 14 October 2008

Abstract Laser is a promising technique used for biopolymer surface modification with micro and/or nano features. In this work, a 193 nm excimer laser was used for poly (ethylene terephthalate) (PET) surfaces chemical patterning. The ablation threshold of the PET film used in the experiments was 62 mJ/cm^2 measured before surface modification. Surface chemical patterning was performed by irradiating PET film in a vacuum chamber filled with ammonia at the flux of 10, 15, 20, 25 ml/min. Roughness of the surface characterized by profilometry showed that there were no significant observed change after modification comparing original film. But the hydrophilicity of the surface increased after patterning and a minimum water contact angle was obtained at the gas flux of 20 ml/min. FT-IR/ATR results showed the distinct amino absorption bands presented at 3352 cm^{-1}and 1613 cm^{-1} after modification and XPS binding energies of C_{1s} at 285.5 eV and N_{1s} at 399.0 eV verified the existence of C–N bond formation on the PET film surface. Tof-SIMS ions mapping used to identify the amine containing fragments corroborates that amino grafting mainly happened inside the laser irradiation area of the PET surface. A hypothesized radical reaction mechanism proposes that the collision between radicals in ammonia and on the PET surface caused by the incident laser provokes the grafting of amino groups.

G. Wu · M. D. Paz · S. Chiussi · J. Serra · P. González · B. Leon
Department of Applied Physics, University of Vigo, Rua Maxwell, Vigo, Spain

G. Wu (✉) · Y. J. Wang
College of Material Science and Engineering, South China University of Technology, Guangzhou, China
e-mail: imwugang@scut.edu.cn

1 Introduction

Surface properties of biopolymers play important roles in the interaction between cells and biomaterials and influence the formation of new tissues and organs around biopolymers [1]. It is reported that cells may react differently to chemical and topographical biopolymer surface stimulus [2, 3]. Thus, manipulating of surface patterning, either physically or chemically, would make a possible to control cells behavior on biopolymer surface for future clinical therapy [4, 5]. Functionalization of biopolymer surfaces is a feasible, simple and economical way to achieve this purpose. However, since most current implanting biopolymers have few reactive chemical groups on their surface, functionalization for them are always complicate or impossible.

Polyethylene terephthalate (PET) has been used as cardiovascular material for long time with the commercial name of Dacron®. Because of thrombus and inflammations related to PET surfaces properties, methods from physical deposition to chemical grafting were studied by many groups in the past several decades to improve that, such as low temperature plasma surface treating [6–8], corona treatment [9–11], micro contact printing [12, 13], ion beam irradiation [14, 15], self assemble monolayer deposition [16, 17], and UV irradiation [18–28].

UV photo surface grafting is the most popular method for PET since the equipment is easy to be assembled. Chemical groups like carboxyl, [18–20] amino, [21] amide, [22, 23] N-vinyl-2-pyrrolidone (NVP), [24] acryl acid, [25, 26] chitosan, [27] hydrophilic PEG, [28] were successfully grafted onto the PET film surface by this method. But since UV lamp has a wide photon spectrum and poor spatial coherence, the grafting efficient is low. Furthermore, some of these experiments [22–26] take place in monomer solution adsorbing undesired remnants of photoinitiators

and homopolymerized polymers [18–22, 27, 28] A promising alternative is using UV lasers with higher chemical selectivity due to their monochromaticity. Other merits of UV laser are fast and direct writing due to its high intensity and spatial confinement.

Lasers are nowadays powerful industrial tool that are widely used to cut from steel to human tissue and to pattern the surface morphology with precise controlled features. Recently, it has been demonstrated that there are certain chemical modifications happened when physical patterning of polymers is performed. [29–32] In fact, during many polymer ablation experiments, the laser activated surface reacts with the surrounding air improving surface hydrophilicity and biocompatibility [29–32].

Following the idea and method of UV lamp irradiation, laser irradiation was used to graft hydroxyethyl methacrylate (HEMA) [33], acrylic acid (AAc) [34–36] and acrylic amide (AAm) [37, 38] onto PET and PP surface through the reaction of laser actived surface with heated monomer solution. However, this complicate reaction is influenced by the solutions and not suitable for fabricating a surface with micro or nano surface chemical features.

In this paper, we proposed and studied a directed UV-laser grafting method for amino surface pattern through the reaction between the dissociated NH_2 radical and the laser activated surface of PET. The PET surface before and after modification was characterized and the grafting mechanism was hypothesized in this paper.

2 Materials and methods

2.1 Materials and laser

PET film with 100 μm thickness was purchased from Esselte. The films were cut into 2 × 2 cm^2 squares and ultrasonic cleaned 10 min in analytic grade methanol, benzene and isopropanol solvent (Sigma Aldrich), respectively and ambient dried in a laminar flow cabinet.

The excimer laser is a Lambda Physik LPX220i ArF laser with pulse duration of 20 ns and a wavelength of 193 nm. The frequency was set to 20 Hz and the energy calibrated by an energy meter (Oriel 70260). The output laser beam was focalized through a rectangular plano-convex lens on the polymer surface placed perpendicular to the incident beam.

2.2 Methods

2.2.1 Surface modification

PET film surface ablation was directly performed in air in order to assess the ablation threshold at air pressure. In the grafting experiments, PET was fixed onto a stage inside a vacuum reaction chamber with a position perpendicular to laser beam. The ammonia (UCAR, electronic grade NH_3) fluxes were controlled by a Bronkhorst F-201D mass flow controller. Pressure was monitored by a capacitance MKS 122B Baratron. The incident energy was adjusted to ensure that no ablation plume could be seen from the PET surface with the ammonia flux at 10 ml/min. This adjusted energy measured before the vacuum window was 20 mJ, a value far below the ablation threshold in air. The distance between the vacuum window and the PET film was 16 cm. The PET film was irradiated for 40 s with the ammonia flux (partial pressure) at 10 (133 Pa), 15 (159.6 Pa), 20 (186.2 Pa) and 25 ml/min (212.8 Pa), respectively.

2.2.2 Profilometry measurement

A surface profilometer (DEKTAK^{3}ST, Veeco) was used to measure the surface roughness and the crater depth after ablation. For the surface roughness determination, the stylus was linearly scanned with soft touch mode both inside and outside the irradiated area over a length of 2000 μm. The horizontal resolution was 1 μm/sample point. Roughness (Ra) values were automatically calculated by the equipment software.

2.2.3 Water contact angle

Static water contact angle measurements were carried out by the water contact meter equipped with CCD detector, dosing control system and related software (CA10+OCA20, Dataphysics). Sessile drop method was used with precisely controlled dosing water volume of 1 μl every time. Measured contact angles were the mean value ± standard error (SE) of five measurements on different parts inside the irradiated spot.

2.2.4 FT-IR/ATR analysis

Infrared spectra were collected using a FT-IR spectrometer (Nicolet 670, Thermo) equipped with the attenuated total reflection (ATR) accessory (IRE: germanium) and a mercury cadmium telluride (MTC) detector. 128 scans were collected between 3600 cm^{-1} and 600 cm^{-1} at 1 cm^{-1} resolution inside and outside the modified spot to obtain the chemical map of the irradiated sample.

2.2.5 XPS analysis

The XPS measurements were carried out using an VG Escalab 250 iXL ESCA instrument (VG Scientific), equipped with a X-ray source providing aluminum $K\alpha_{1,2}$ monochromatized radiation at 1486.92 eV. Photoelectrons

were collected from a take off angle of 90° relative to the sample surface. The measurements were done in a Constant Analyser Energy mode (CAE) with a 100 eV pass energy for survey spectra and 20 eV pass energy for high resolution spectra. Surface charge was neutralized and charge referencing was done by setting the lower binding energy C_{1s} hydrocarbon peak at 285.0 eV. Surface elemental composition was determined using the standard Scofield photoemission cross sections.

2.2.6 Tof-SIMS analysis

The mass spectra of the samples were recorded on a TOF-SIMS IV instrument from Ion-Tof GmbH. The sample was bombarded with a pulsed Gallium ion beam. The secondary ions generated were extracted with a 10 kV voltage and their time of flight from the sample to the detector was measured in a reflection mass spectrometer. Analysis conditions for this work were: 25 keV pulsed Ga^+ beam at 45° incident, rastered over 500 × 500 μm. Electron flood gun charge compensation was necessary during measurements.

3 Results and discussion

3.1 Calculation of reaction parameters

Table 1 shows the parameters used for the laser irradiation experiments. Since the experiments were performed inside the vacuum chamber, parameters must be corrected according to the vacuum degree. The nominal ammonia gas flow speed $V_{\text{corrected}}^{\text{ammonia}}$ between pulses, ammonia concentration C_{ammonia} and the number of the photons arriving to the polymer surface were calculated according to the following equations, respectively. The ammonia was supposed to behave as an ideal gas.

$$V_{\text{corrected}}^{\text{ammonia}} = \frac{P_{\text{gauge}} Q_{\text{gauge}}}{PS} \quad (1)$$

$$C_{\text{ammonia}} = \frac{P}{RT} \quad (2)$$

$$N_{\text{photons}} = \frac{I}{h\nu} = \frac{I_0}{h\nu} e^{-n\sigma t} = \frac{I_0 \lambda}{hc} e^{-\frac{N_{AV} P \sigma t}{RT}} \quad (3)$$

whereby P_{gauge} is the pressure used for the flux meter calibration, Q_{gauge} is the ammonia flux read from the flux meter, P is the chamber working pressure, I_0 is the incident laser energy, S is the cross section area of the vacuum chamber, λ is the laser wavelength, t is the distance from the chamber window to the sample surface, σ is the ammonia absorption cross section at 193 nm (1E-17 cm^2) [39], h is the Planck constant, N_{AV} is the Avogadro constant, c is light speed, R is 8.314 kJ/mol and T here is the temperature (293.15 K).

In this experiment, the nominal ammonia flow speed, vacuum chamber pressure and the ammonia concentration in the chamber all increased with the rising of ammonia fluxes. The photon numbers arriving to the matrix surface decreased with increasing ammonia flux.

The maximum nominal flow speed of the ammonia calculated in the vacuum chamber is 135 μm/50 ms, far lower than the irregular Brownian movement of the gas molecules. So the ammonia gas filled the entire chamber in the experiment according to this result. This basic idea was used to calculate the ammonia concentration in the chamber.

3.2 Ablation threshold

The onset of polymer laser ablation is caused by photon energy absorbing photochemically and photothermally. The ablation rate in air (Δd) versus the logarithms of the incident fluence (F_0) was plotted in Fig. 1. The ablation threshold and the absorption coefficient of the material were calculated from Fig. 1 as the Ref. [40]. The extrapolated fluence at zero ablation rate, also known as ablation threshold (F_t) can be assessed in our experiment to be 62 mJ/cm^2 and the calculated absorption coefficient to be 5.6 μm^{-1}. These values are slightly different from those obtained in Ref. [41]. This could be the reason attributed to their shorter pulse length and different PET purchased from other providers.

In the surface chemical modification, since the grafted groups would be removed by the ablation, it is important to keep the fluence under the ablation threshold to avoid possible removal of polymer molecules and/or grafted groups from the surface. Therefore, the surface grafting

Table 1 Parameters of the laser irradiation grafting

	Flux(Q_{gauge}) (ml/min)	$V_{\text{corrected}}^{\text{ammonia}}$ (μm/50 ms)	P_{Vacuum} (Pa)	C_{ammonia} (mol/m^3)	N_{photons}
A	10	85	133	5.46E-2	2.3713E20
B	15	105	159.6	6.55E-2	9.76735E19
C	20	125	186.2	7.64E-2	4.02316E19
D	25	135	212.8	8.73E-2	1.65714E19

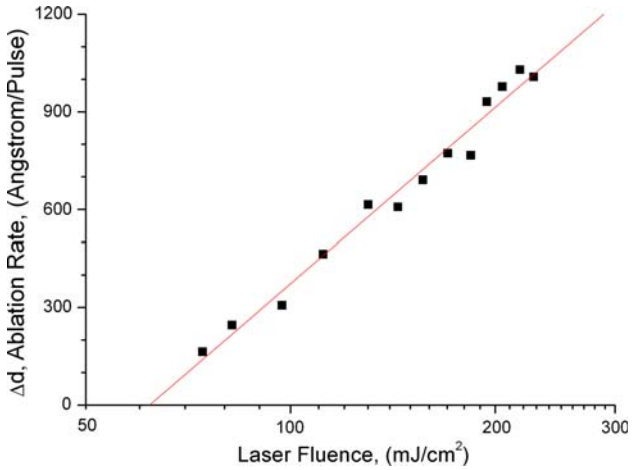

Fig. 1 Ablation rate versus laser incident fluence for PET in air

experiments were performed at a relative lower fluence of 30 mJ/cm^2. It is important to remind that the ablation experiments were done in air but not in the ammonia reactive gas used for chemical grafting.

3.3 Surface water contact angle and roughness

Figure 2 shows the influence of the ammonia flux on the water contact angle and surface roughness. The water contact angle decreased with the increasing ammonia flux and obtained its minimum value at a flux of 20 ml/min. No significant change of surface roughness could be observed after laser irradiation in all ammonia fluxes.

Water contact angle can be easily used to check the possible change of the surface caused chemically or/and physically. Since the surface roughness did not change in all the experiments, the decreasing of the water contact angle must be mainly caused by the surface chemical change. The lower water contact angle implies that more hydrophilic molecules were grafted onto the PET surface after laser irradiation in ammonia gas.

In this research, the grafting of hydrophilic molecules could be the result of reactions between ammonia gas radicals and polymer surface radicals caused by photon dissociation.

The energy of 193 nm photons and the main chemical bonds of PET are displayed in Fig. 3. The energy of the photon is higher than most chemical bonds except the aromatic hydrogen and carboxyl bonds. This enables each photon to decompose those lower energetic bonds through single photon absorption. Taking into account the high density of photons in laser processing, the higher energy bonds can be broken through multiphoton absorption. Reactions will then occur between the photon activated surface groups and the ambient species or between active groups themselves. Moreover, ammonia has a strong capability to absorb the 193 nm laser photons and to decompose into $NH_2^\bullet$ and $H^\bullet$ radicals [39]. $NH_2^\bullet$ radicals reaction with the PET surface radicals could be the main reason for the improvement of the hydrophilicity of the surface obtained in this experiment. On the other hand, this effect might be strengthened due to the reactions of the $H^\bullet$ radicals with the remaining $NH_3^\bullet$ molecules producing additional $NH_2^\bullet$ radicals and $H_2^\bullet$ as well as with the original PET surfaces stripping H atoms an forming PET$^\bullet$ and H_2 molecules.

By increasing the flux, i.e. increasing the pressure and concentration, the photon absorption in the gas increased. This made a reduction of the incident photons arriving PET surface (Table 1). Thus, at higher gas flux, more radicals are produced in the gas and less radicals are excited on the surface. Proper gas flux seems to balance the radicals formation in gas and on matrix surface to achieve the best

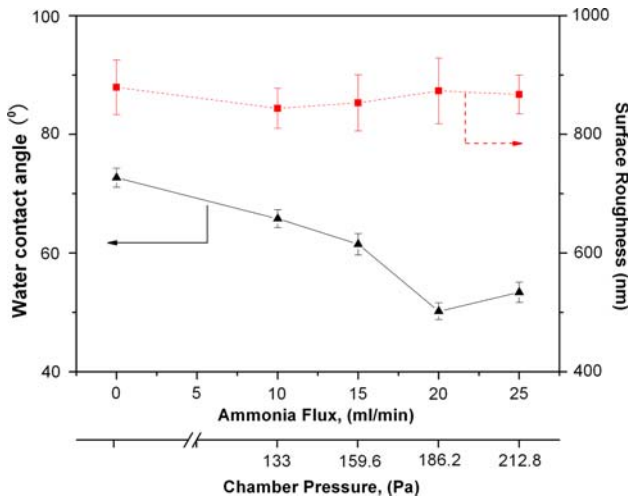

Fig. 2 Influence of ammonia flux on water contact angle and surface roughness

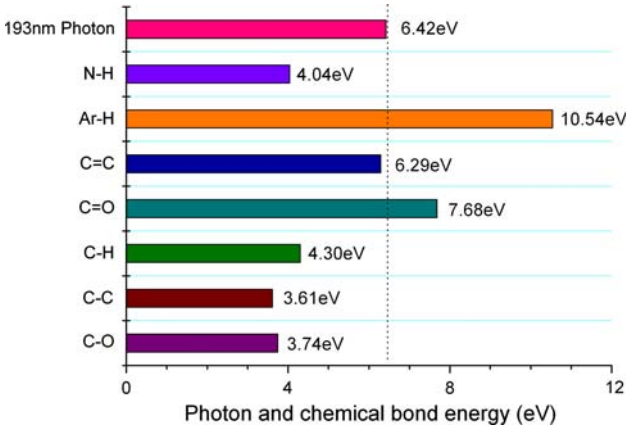

Fig. 3 Energy of 193 nm photon and main chemical bonds in PET

hydrophilicity and the maximum grafting ratio, which appears at 20 ml/min.

3.4 FT-IR/ATR analysis

The spectra of PET before and after modification in different ammonia flux were obtained by FT-IR/ATR shown in Fig. 4. Before modification, absorption bands belonging to different C–H bonds were found. Those bands were at 3060 cm^{-1} belonging to phenyl C–H stretching vibration, at 2926 cm^{-1}, 2847 cm^{-1} and 1473 cm^{-1} assigned to the asymmetric, anti-asymmetric stretching, vibration and the scissors bending vibration of $–CH_2–$, and at 2962 cm^{-1} belonging to $–CH_3$ the asymmetric vibration [42]. After modification, almost all of them decreased or disappeared except the $–CH_3$ absorption band. Furthermore, new absorption bands at 3352 cm^{-1} and 1613 cm^{-1} assigned to the distinct stretching vibration and scissors bending vibration of $–NH_2$ appeared in the spectra demonstrating that $–NH_2$ was grafted onto the surface after irradiation [43, 44].

The decreasing of $–CH_2–$ and phenyl C–H bands implies that de-hydrogen reactions happened at those aromatic and aliphatic sites. These de-hydrogenated carbon atoms could be the reaction centers for the grafting of $–NH_2$ in ammonia gas. The amino groups should therefore graft onto both aromatic and aliphatic segments.

Methyl group absorption (2962 cm^{-1}) without significant intensity change was observed in FT-IR/ATR before and after laser irradiation. This is due to the residual methyl in the original PET and those by products after laser processing. During that processing, the main chain breaking in PET can produce the $–CH_2^{\bullet}$ radicals. These radicals might react with the $H^{\bullet}$ radicals produced in the ammonia gas and result in the formation of a new terminate methyl group in PET. If the reaction radicals in the gas are $NH_2^{\bullet}$ instead of $H^{\bullet}$, the amino would be the terminate group in PET.

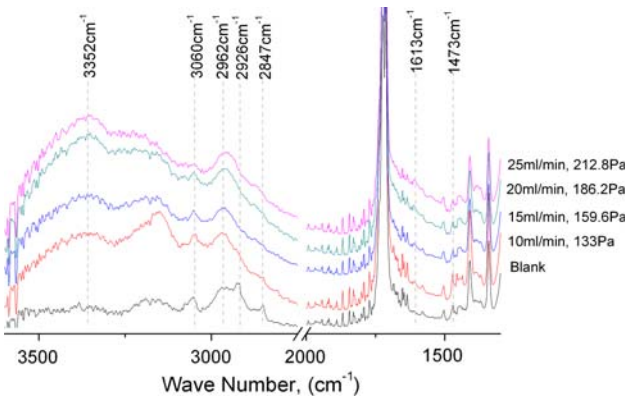

Fig. 4 FT-IR/ATR spectra of PET film surface in different ammonia flux condition

3.5 XPS analysis

Figure 5 displays the spectra of PET film surface after modification. In this figure, binding energy of C_{1s}, N_{1s} and O_{1s} presented at 284.98, 399.00 and 532.00 eV respectively [45]. PET doesn't contain nitrogen molecular theoretically. The nitrogen displayed in this figure therefore was introduced by the laser processing in ammonia atmosphere.

XPS atomic composition of the modified PET film surface was shown in Table 2. It displays that the C_{1s} increased and O_{1s} as well as O/C decreased with decreasing of ammonia flux. On the other hand, the N_{1s} and N/C ratio increased with increasing of the flux, reaching its maximum value at flux of 20 ml/min.

XPS is a sensitive surface characterization method used to get important chemical information of the materials surface in a depth of several tenths of nanometers and the quantificational data can be used to compare the chemical composition changes on the surface. The increasing of C_{1s} and decreasing of O_{1s} suggested that a decarbonylation might happen during PET modification in ammonia gas. This phenomenon is quite similar to that reported in PET ablation in He gas where decarbonylation is the predominant detected phenomenon [41, 46]. That means in this process, small molecules like CO_2, CO were extracted from

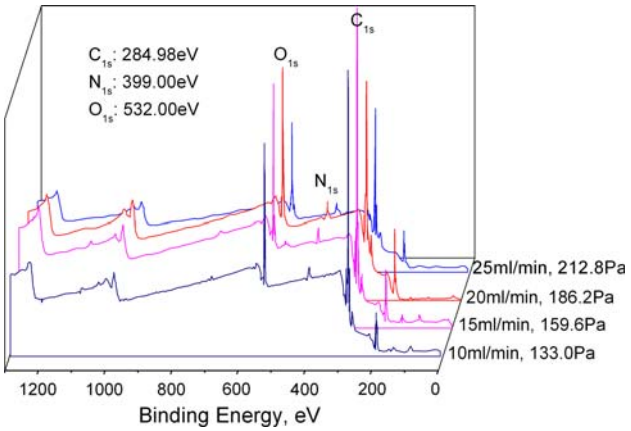

Fig. 5 XPS spectrum of PET after 193 nm laser irradiation in ammonia gaseous

Table 2 Atom percentage and relative ratio after modification

Ammonia flux	C_{1s}	O_{1s}	O/C	N_{1s}	N/C
Original	71.4	28.6	0.401		
25 ml/min	72.8	23.4	0.321	3.8	0.0525
20 ml/min	73.5	22.1	0.301	4.4	0.0600
15 ml/min	79.1	18.0	0.227	2.9	0.0367
10 ml/min	79.8	17.2	0.216	3.0	0.0376

the PET surface causing the formation of the terminate free radicals on the surface.

The maximum N_{1s} and N/C were observed at ammonia flux of 20 ml/min, the same flux that produced a minimum water contact angle (Fig. 1). This is again an indication that a balance between the activated radicals on the PET surface and in the ammonia gas occurs, as explained before.

The types of different chemical bonds after the modification could be determined by high resolution C_{1s} and N_{1s} XPS spectra as those displayed in Fig. 6. The C_{1s} peak for the modified PET film was resolved into five main component peaks of different carbon types: Hydrocarbon or carbon bond (*C*–H/*C*–C) at 284.8 eV, carbonyl carbon (–*C*–O–) at 288.5 eV, ether carbon (–*C*=O) at 286.7 eV, aliphatic amine carbon (–*C*–N–) at 285.5 eV and aromatic amine carbon at 283.9 eV [47–49]. The N_{1s} peak could also be resolved into two different nitrogen types, the amine nitrogen connected to the PET aromatic and the aliphatic segments, displayed at 398.9 eV and 401.2 eV, respectively [50–52]. The C–N bond energy corresponds to the amine groups grafted onto the two possible aromatic and aliphatic carbon sites as also deduced from the FT-IR/ATR results.

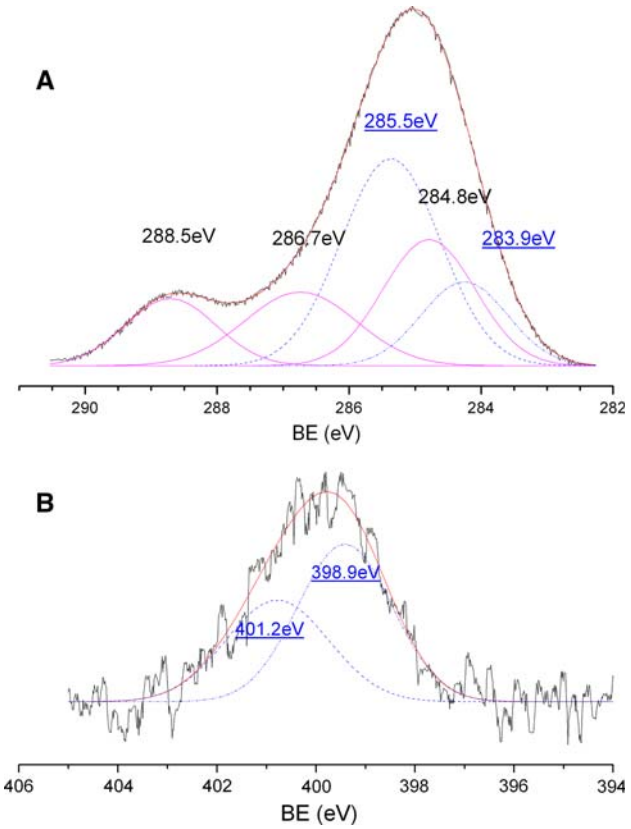

Fig. 6 High resolution binding energy of C_{1s} and N_{1s} of treated PET in ammonia atmosphere

Table 3 displayed the calculated peak areas of resolved C–N bonds curve in C_{1s} and N_{1s} high resolution XPS spectra. The maximum values were found again at a flux of 20 ml/min. The difference between the maximum and minimum area (A_{20}–A_{10}) obtained with samples modified using 20 ml/min and 10 ml/min, displayed that the C–N grafting on aromatic segments was more influenced by the ammonia flux than the grafting on aliphatic segments. Since the breaking of the phenyl C–H bond was possibly caused by a multi photon absorption mechanism, the result suggest that the ammonia gas absorption would more likely influence the multi photon activation of the molecular chemical bonds. This fact could be used to selectively activate the chemical bond in a controlled mode.

3.6 Tof-SIMS analysis

The amino grafted PET was also characterized by Tof-SIMS as those shown in Fig. 7. The positive Tof-SIMS spectra of

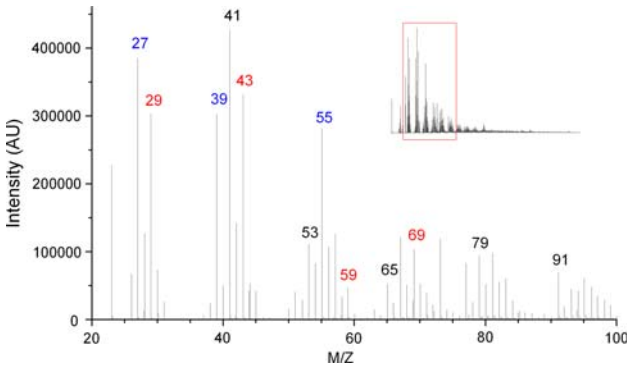

Fig. 7 Positive Tof-SIMS spectrum of PET after modification

Table 3 Area calculation of fitted line in high resolution C_{1s} and N_{1s} spectra of XPS

Ammonia flux	Aliphatic		Aromatic	
	C–N (285.5 eV)	C–*N* (401.2 eV)	*C*–N (283.9 eV)	C–*N* (398.9 eV)
25 ml/min	379.06	11.835	215.08	43.677
20 ml/min	422.66	36.364	261.56	66.408
15 ml/min	350.14	32.874	103.82	32.043
10 ml/min	318.68	9.948	91.535	26.478
A_{20}–A_{10}	103.98	26.416	170.025	39.93

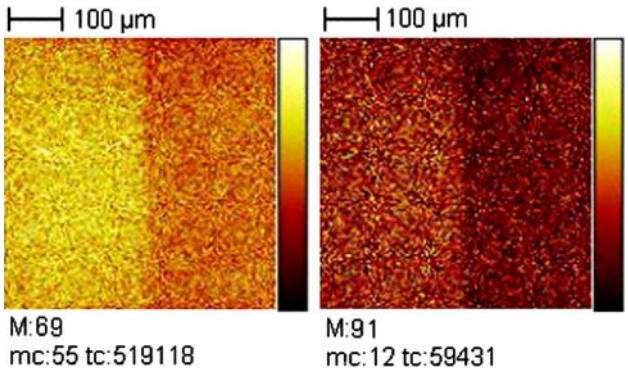

Fig. 8 Tof-SIMS positive fragments mapping of modified PET (right part was modified)

the treated PET showed the major peaks at: M/Z 29/30, 43/44, 59/60, 69/70, which were assigned to $CH(NH_2)^+$/$CH(NH_2)^+$, $CH_2CH(NH_2)^+$/$CH_2CH(NH_2)^+$, $OCH(NH_2)^+$/$OCH_2(NH_2)^+$ and $OCH_2CH(NH_2)^+$/$OCH(NH_2)CH_2^+$/$OCH_2(NH_2)CH_2^+$/$OCH_2CH_2(NH_2)^+$, respectively. These fragments could come from the amine grafted aliphatic PET segments. M/Z peaks at 28, 40/41, 53/54, 65/66, 78/79/80 and 91/92 were assigned to $C(NH_2)^+$, $C(NH_2)C^+$/$C(NH_2)CH^+$, $C(NH_2)CHC^+$/$CC(NH_2)CH^+$, $CC(NH_2)CHC^+$/$C(NH_2)CHCCH^+$, $C(NH_2)CHCCHCH^+$/$CC(NH_2)CHCCH^+$/$C(NH_2)CHCHCHCH^+$, $C(NH_2)CHCCHCHC^+$/$C(NH_2)CHCCHCHCH^+$, which could come from the amine grafted aromatic PET segments. A Tof-SIMS spectrum contains the chemical information of only several nanometers depth and precisely represents the surface chemical structure. The results clearly indicate that the amino groups were grafted on to the polymer molecules both on the aromatic and aliphatic segments.

Tof-SIMS mapping was performed in an area of a 500 × 500 μm^2 square for analyzing both the irradiated and unirradiated surfaces, as displayed in Fig. 8. Through surface scanning and collecting the specific fragments ions from the surface, local surface chemistry maps were visualized and used to distinguish the difference between the modified and un-modified part on the surface. The amine containing fragments with the specific mass M/Z: 69, 91 were chosen as the mapping ions. The maps showed the expected border line in the middle of the image, clearly separating the modified and unmodified areas. Only the irradiated and modified area (right part) contains the ions used for mapping as that can be distinguished from the significant color difference between two parts.

Figure 8 also evidences that the surface grafting mainly happened inside the irradiated area. Although free radicals

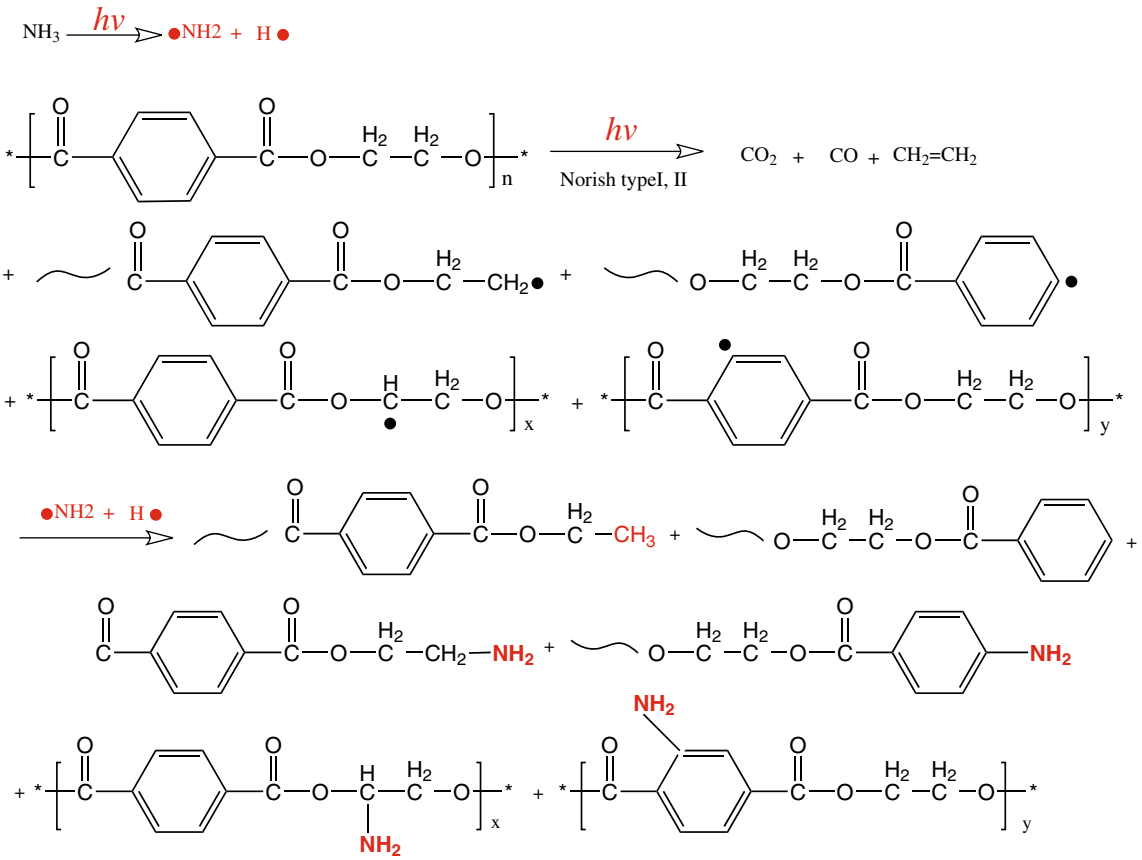

Scheme 1 Mechanism of laser induced amino grafting

produced in the ammonia gas have the potential and possibility to initiate the hydrogen abstraction from the polymer molecule and to form radicals on the surface, this mechanism seems to be less important. The main reason for the surface chemical grafting seems to be the laser activation of both, the surface and the ammonia gas.

3.7 Mechanism of laser induced grafting

Scheme 1 shows a possible reaction mechanism, radicals in ammonia gas and on PET surface are excited by single or multiple laser photon absorption. The ammonia radicals impact on the PET film surface and react with radicals on the film resulting in the amino groups grafting.

The absorbed photons in the PET caused two types of bond breaking phenomena, Norrish type I and II [53]. In Norrish type II, the main molecular chain C–C and C–O bonds are broken, while in Norrish type I, both C–H at aromatic and aliphatic parts are decomposed. As reported in the literature, Norish type I decomposition easily happens during low energy irradiation [41]. Therefore, the amino group could have more possibility to be grafted as the pendant group when low energy irradiation is used. In the same procedure, hydrogen radicals' collision with the radicals on the polymer surface can be considered as a competitive side reaction which will influence the amine grafting.

4 Conclusion

Different ammonia fluxes during the laser irradiation processing have been investigated with respect to their influence on the amine grafting efficiency. All the results showed that the amino groups were successfully grafted onto the PET film surface inside the irradiated area. We attribute this to the radical reaction caused by the laser decomposed ammonia radicals and those on the PET film surface, allowing the subsequent introduction of amino groups.

To adjust proper ammonia flux is important for balancing the radical production between ammonia and PET film surface and for getting the highest amino grafting ratio. Higher flux and lower flux will decrease the radicals produced on the film surface and in the ammonia atmosphere, respectively and thus reduce the amino grafting.

The surface modification of PET with reactive chemical covalent amine bonds is very attractive and highly desirable for biomedical applications. Using Laser as an alternative tool can provide selective surface grafting in areas without using any contact photo masks. This provides a versatile and simple tool for the biopolymers surface chemical mapping.

Combining the surface morphology patterning and chemical mapping together, laser irradiation may be an economical technique to fabricate an ideal biosurface with micro or nano features by the same machine and even in one single processing step. This makes laser a promising tool in the biopolymer surface modification in the future.

Acknowledgements This research was financial supported by the EU project: PROTEUS, INTERREG III A—SP1.P151/03, Spain project: BIOAVAN, PSE 300100-206 and NSFC project: 50403023. We appreciate Dr. Carmen Serra from CACTI of University of Vigo for Tof-SIMS and XPS, Yan Leping from South China University of Technology for FT-IR/ATR measurements.

References

1. P. Vadgama, Surface biocompatibility. Annu. Rep. Prog. Chem. Sect. C **101**, 14–52 (2005). doi:10.1039/b408906p
2. A. Stevens, L. Gaard-Andersen, Making waves: pattern formation by a cell-surface-associated signal. Trends Microbiol. **13**, 249–252 (2005). doi:10.1016/j.tim.2005.04.002
3. D.R. Jung, R. Kapur, T. Adams, K.A. Giuliano, M. Mrksich, H.G. Craighead, D.L. Taylor, Topographical and physicochemical modification of material surface to enable patterning of living cells. Crit. Rev. Biotechnol. **21**, 111–154 (2001). doi:10.1080/20013891081700
4. Y.X. Wang, J.L. Robertson, J. Spillman, R.O. Claus, Effects of the chemical structure and the surface properties of polymeric biomaterials on their biocompatibility. Pharm. Res. **21**, 1362–1373 (2004). doi:10.1023/B:PHAM.0000036909.41843.18
5. I. Taniguchi, W.A. Kuhlman, A.M. Mayes, L.G. Griffith, Functional modification of biodegradable polyesters through a chemoselective approach: application to biomaterial surfaces. Polym. Int. **55**, 1385–1397 (2006). doi:10.1002/pi.2139
6. J. Tang, Q. He, H. Chen, N. He, Synthesis and hybridization studies of DNA on functionalized polypropylene surfaces. J. Nanosci. Nanotechnol. **5**, 1225–1229 (2005). doi:10.1166/jnn.2005.222
7. N. Inagaki, K. Narushima, K. Kuwabara, K. Tamura, Introduction of amino functionalities on ethylene-co-tetrafluoroethylene film surfaces by NH_3 plasmas. J. Adhes. Sci. Technol. **19**, 1189–1205 (2005). doi:10.1163/156856105774429064
8. A. Musyanovych, H.J.P. Adler, Grafting of amino functional monomer onto initiator-modified polystyrene particles. Langmuir **21**, 2209–2217 (2005). doi:10.1021/la047960+
9. L.P. Zhu, B.K. Zhu, L. Xu, Y.X. Feng, F. Liu, Y.Y. Xu, Corona-induced graft polymerization for surface modification of porous polyethersulfone membranes. Appl. Surf. Sci. **253**, 6052–6059 (2007). doi:10.1016/j.apsusc.2007.01.004
10. S.J. Park, J.S. Jin, Effect of corona discharge treatment on the dyeability of low-density polyethylene film. J. Colloid Interface Sci. **236**, 155–160 (2001). doi:10.1006/jcis.2000.7380
11. N. Dumitrascu, T. Balau, M. Tasca, G. Popa, Corona discharge treatment of the plastified PVC films obtained by chemical grafting. Mater. Chem. Phys. **65**, 339–344 (2000). doi:10.1016/S0254-0584(00)00261-3
12. J. Kim, J. Park, S. Lee, D. Sohn, Surface-grafting of polyglutamate on Si wafer using micro contact printing. Mol. Cryst. Liq. Cryst. **464**, 211–216 (2007). doi:10.1080/15421400601031017
13. W.M. Lackowski, P. Ghosh, R.M. Crooks. Micron-scale patterning of hyperbranched polymer films by micro-contact printing. J. Am. Chem. Soc. **121**, 1419–1420 (1999). doi:10.1021/ja983545q

14. M.L. Carbajal, E.E. Smolko, M. Grasselli, Oriented immobilization of proteins on grafted porous polymers. Nucl. Instrum. Methods Phys .Res. B **208**, 416–423 (2003). doi:10.1016/S0168-583X(03)00988-1
15. V. Švorčík, K. Prošková, V. Hnatowicz, V. Rybka, Alanine grafting of ion-beam-modified polyethylene. J. Appl. Polym. Sci. **75**, 1144–1148 (2000). doi:10.1002/(SICI)1097-4628(20000228)75:9<1144::AID-APP7>3.0.CO;2-3
16. K. Rajangam, H.A. Behanna, M.J. Hui, X. Han, J.F. Hulvat, J.W. Lomasney, S.I. Stupp, Heparin binding nanostructures to promote growth of blood vessels. Nano. Lett. **6**, 2086–2090 (2006). doi:10.1021/nl0613555
17. A.K. Chakraborty, A.J. Golumbfskie, Polymer adsorption-driven self-assembly of nanostructures. Annu. Rev. Phys. Chem. **52**, 537–573 (2001). doi:10.1146/annurev.physchem.52.1.537
18. Q. Zhao, C. Wan, J. Liu, K. Qiu, Research in synthesis of bioactive peptide RGD and the method for its grafting on PET surface. Sheng Wu Yi Xue Gong Cheng Xue Za Zhi. J. Biomed. Eng. **20**, 384–387 (2003)
19. Z. Zhu, M.J. Kelley, Poly(ethylene terephthalate) surface modification by deep UV (172 nm) irradiation. Appl. Surf. Sci. **236**, 416–425 (2004). doi:10.1016/j.apsusc.2004.05.012
20. C. Chollet, S. Lazare, C. Re, F. Guillemot, R. Bareille, M.C. Durrieu, RGD peptides micro-patterning on?poly(ethylene terephthalate) surfaces. ITBM-RBM **28**, 2–12 (2007)
21. T. Sugawara, T. Matsuda, Novel surface graft copolymerization method with micron-order regional precision. Macromolecules **27**, 7809–7814 (1994). doi:10.1021/ma00104a040
22. A. Wirsén, H. Sun, A.C. Albertsson, Solvent-free vapor-phase photografting of acrylamide onto poly(ethylene terephthalate). Biomacromolecules **6**, 2697–2702 (2005). doi:10.1021/bm050169a
23. Z.P. Yao, B. Ranby, Surface modification by continuous graft copolymerization. III. Photoinitiated graft copolymerization onto poly(ethylene terephthalate) fiber surface. J. Appl. Polym. Sci. **41**, 1459–1467 (1990). doi:10.1002/app.1990.070410709
24. K.S. Chen, Y.A. Ku, H.R. Lin, T.R. Yan, D.C. Sheu, T.M. Chen, Surface grafting polymerization of JV-Vinyl-2-pyrrolidone onto a poly(ethylene terephthalate) nonwoven by plasma pretreatment and its antibacterial activities. J. Appl. Polym. Sci. **100**, 803–809 (2006). doi:10.1002/app.23111
25. C. Wu, J. Zhao, B. Zhang, M. Yuan, Surface graft polymerization of PET and PE fibers by UV irradiation. J. Dong Hua Univ. **15**, 38–41 (1998). English Edition
26. Y.W. Song, H.S. Do, H.S. Joo, D.H. Lim, S. Kim, H.J. Kim, Effect of grafting of acrylic acid onto PET film surfaces by UV irradiation on the adhesion of PSAs. J. Adhes. Sci. Technol. **20**, 1357–1365 (2006). doi:10.1163/156856106778456564
27. J. Wang, P. Li, H. Sun, P. Yang, Y.X. Leng, J.Y. Chen, N. Huang, Blood compatibility of chitosan immobilized on poly(ethylene terephthalate) surface modified by plasma and ultraviolet grafting. Key Eng. Mater. **288–289**, 327–330 (2005)
28. E. Uchida, Y. Uyama, Y. Ikada, Grafting of water-soluble chains onto a polymer surface. Langmuir **10**, 481–485 (1994). doi:10.1021/la00014a023
29. H. Watanabe, M. Yamamoto, Chemical structure change of a KrF-laser irradiated PET fiber surface. J. Appl. Polym. Sci. **71**, 2027–2031 (1999). doi:10.1002/(SICI)1097-4628(19990321)71:12<2027::AID-APP12>3.0.CO;2-K
30. J.S. Rossier, P. Bercier, A. Schwarz, S. Loridant, H.H. Girault, Topography, crystallinity and wettability of photoablated PET surfaces. Langmuir **15**, 5173–5178 (1999). doi:10.1021/la9809877
31. T. Lippert, T. Nakamura, H. Niino, A. Yabe, Laser induced chemical and physical modifications of polymer films: dependence on the irradiation wavelength. Appl. Surf. Sci. **109–110**, 227–231 (1997). doi:10.1016/S0169-4332(96)00663-0
32. D. Knittel, E. Schollmeyer, Surface structuring of synthetic fibres by UV laser irradiation. Part III. Surface functionality changes resulting from excimer-laser irradiation. Polym. Int. **45**, 103–109 (1998). doi:10.1002/(SICI)1097-0126(199801)45:1<103::AID-PI917>3.0.CO;2-2
33. M.T. Khorasani, H. Mirzadeh, P.G. Sammes, Laser surface modification of polymers to improve biocompatibility: HEMA grafted PDMS, in vitro assay - III. Radiat. Phys. Chem. **55**, 685–689 (1999). doi:10.1016/S0969-806X(99)00212-1
34. H. Mirzadeh, A.R. Ekbatani, A.A. Katbab, Surface modification of ethylene-propylene rubber by laser grafting of acrylic acid. Iranian Polym. J. **5**, 225–230 (1996). English Edition
35. W. Kesting, D. Knittel, E. Schollmeyer, Surface modification of polymer fibres by UV laser irradiation. X. UV-laser-induced graft copolymerization of acrylic acid onto polypropylene. Angewandte Makromolekulare Chemie. **182**, 177–186 (1990). doi:10.1002/apmc.1990.051820112
36. H. Mirzadeh, M. Dadsetan, N. Sharifi-Sanjani, Platelet adhesion on laser-induced acrylic acid-grafted polyethylene terephthalate. J. Appl. Polym. Sci. **86**, 3191–3196 (2002). doi:10.1002/app.10775
37. M. Dadsetan, H. Mirzadeh, N. Sharifi-Sanjani, Surface modification of polyethylene terephthalate film by CO2 laser-induced graft copolymerization of acrylamide. J. Appl. Polym. Sci. **76**, 401–407 (2000). doi:10.1002/(SICI)1097-4628(20000418)76:3<401::AID-APP15>3.0.CO;2-S
38. H. Mirzadeh, A.A. Katbab, R.P. Burford, CO2-pulsed laser induced surface grafting of acrylamide onto ethylene-propylene rubber (EPR). II. Radiat. Phys. Chem. **42**, 53–56 (1993). doi:10.1016/0969-806X(93)90201-5
39. I.P. Herman, Laser-assisted deposition of thin films from gas-phase and surface-adsorbed molecules. Chem. Rev. **89**, 1323–1357 (1989). doi:10.1021/cr00096a005
40. Y.T. Chen, K. Naessens, R. Baets, Y.S. Liao, A.A. Tseng, Ablation of transparent materials using excimer lasers for photonic applications. Opt. Rev. **12**, 427–441 (2005). doi:10.1007/s10043-005-0427-x
41. H. Watanabe, M. Yamamoto, Laser ablation of poly(ethylene terephthalate). J. Appl. Polym. Sci. **64**, 1203–1209 (1997). doi:10.1002/(SICI)1097-4628(19970509)64:6<1203::AID-APP21>3.0.CO;2-V
42. J. Kim, D. Jung, Y. Park, Y. Kim, D.W. Moon, T.G. Lee, Quantitative analysis of surface amine groups on plasma-polymerized ethylenediamine films using UV-visible spectroscopy compared to chemical derivatization with FT-IR spectroscopy, XPS and TOF-SIMS. Appl. Surf. Sci. **253**, 4112–4118 (2007). doi:10.1016/j.apsusc.2006.09.011
43. I.M. El Nahhal, M.M. Chehimi, C. Cordier, G. Dodin, XPS, NMR and FTIR structural characterization of polysiloxane-immobilized amine ligand systems. J. Non-Cryst. Solids **275**, 142–146 (2000). doi:10.1016/S0022-3093(00)00243-X
44. K.S. Siow, L. Britcher, S. Kumar, H.J. Griesser, Plasma methods for the generation of chemically reactive surfaces for biomolecule immobilization and cell colonization - A review. Plasma Process. Polym. **3**, 392–418 (2006). doi:10.1002/ppap.200600021
45. P. Laurens, S. Petit, F. Refi-Khonsari, Study of PET surfaces after laser or plasma treatment: surface modifications and adhesion properties towards Al deposition. Plasmas Polym. **8**, 281–295 (2003). doi:10.1023/A:1026337227361
46. M.K. Shi, G. Dunham, M.E. Gross, G.L. Graff, P.M. Martin, Plasma treatment of PET and acrylic coating surfaces - I. In-situ XPS measurements. J. Adhes. Sci. Technol. **14**, 1485–1498 (2000). doi:10.1163/156856100742320
47. W. Li, E. Ding, Characterization of PET fabrics surface modified by graft cellulose nano-crystal using TGA, FE-SEM and XPS. Surf. Rev. Lett. **13**, 819–823 (2006). doi:10.1142/S0218625X06008906

48. N.W. Hayes, G. Beamson, D.T. Clark, D.S.L. Law, R. Raval, Crystallisation of PET from the amorphous state: observation of different rates for surface and bulk using XPS and FTIR. Surf. Interface Anal. **24**, 723–728 (1996). doi:10.1002/(SICI)1096-9918(19960930)24:10<723::AID-SIA186>3.0.CO;2-Y
49. L.N. Bui, M. Thompson, N.B. McKeown, A.D. Romaschin, P.G. Kalman, Surface modification of the biomedical polymer poly(ethylene terephthalate). Analyst (Lond) **118**, 463–474 (1993). doi:10.1039/an9931800463
50. C. Jie-Rong, W. Xue-Yan, W. Tomiji, Wettability of poly(ethylene terephthalate) film treated with low-temperature plasma and their surface analysis by ESCA. J. Appl. Polym. Sci. **72**, 1327–1333 (1999). doi:10.1002/(SICI)1097-4628(19990606)72:10<1327::AID-APP13>3.0.CO;2-0
51. F.R. Lang, Y. Pitton, H.J. Mathieu, D. Landolt, E.M. Moser, Surface analysis of polyethyleneterephthalate by ESCA and TOF-SIMS. Fresenius. J. Anal. Chem. **358**, 251–254 (1997). doi:10.1007/s002160050398
52. M. Farber, F. Huisken, Intracluster reactions: the formation of hydrazine complexes from ammonia clusters following ArF excimer laser excitation. J. Chem. Phys. **104**, 4865–4868 (1996). doi:10.1063/1.471155
53. Y.G. Yingling, B.J. Garrison, Coarse-grained model of the interaction of light with polymeric material: onset of ablation. J. Phys. Chem. B **109**, 16482–16489 (2005). doi:10.1021/jp0527711